COBEM 2021 26th International Congress of Mechanical Engineering
ABCM Associação Brasileira de Engenharia e Ciências Mecânicas
November 22-26, 2021, Virtual Congress, Brazil

COB-2021- 2263
QUALITY INSPECTION USING ACTIVE INFRARED THERMOGRAPHY WITH COMPUTATIONAL VISION AID USED IN COMPOSITE MATERIAL OF WIND TURBINE BLADE
26th COBEM

Júlio César Capistrano Estácio
julioc.estacio@gmail.com
Darlan Almeida Barroso
darlan.engemec@gmail.com
Marcello Carvalho dos Reis
mcarv.reis@gmail.com
Jessyca Almeida Bessa
bessa.jessyca@ifce.edu.br
Auzuir Ripardo de Alexandria
Instituto Federal de Educação, Ciência e Tecnologia do Ceará
auzuir@ifce.edu.br

Abstract. *The renewable energy sources appear as alternatives that do not pollute the atmospheric air, avoiding the emission of gases that cause the greenhouse effect, among other benefits such as the inexhaustible availability of these sources. Infrared thermography has gained important prominence among the non-destructive tests used in the quality control of wind turbine blades (Wind Turbine Blades – WTB). Some decades, a global trend for has been the use of the concept of total quality, which attributes benefits such as zero-defect manufacturing, productivity gains, elimination of unnecessary costs, in addition to allowing greater safety, which is why it is a very popular concept. by the aerospace industry. One of the biggest challenges in wind blade inspections to reach total quality is the implementation of inspection tasks along the production line through computer vision. This work proposes the use of an active infrared thermography method with the aid of a computer vision system to identify defects in samples of the Glass Fiber Reinforced Polymer (GFRP) composite used in the manufacture of wind turbine blades. Algorithms implemented in Python programming language are used with the help of routines from the OpenCV library to detect internal defects varying diameters and depths. The results of an experimental test are evaluated to validate the implemented computer vision system, observing the performance of the techniques used.*

Keywords: *infrared thermography, quality inspection, wind turbine blades, thermography imaging, computer vision.*

1. INTRODUCTION

Wei (2020) states that the world is currently facing urgent and crucial environmental and resource crises, such as carbon emissions, air pollution and energy shortages, which need to be addressed for long-term sustainable economic development. China, to address these issues and fulfill its commitment to the Paris Climate Agreement, is transitioning from fossil fuels such as coal as an energy source to renewable energy by identifying offshore wind energy as a strategic emerging industry. Investments in wind energy, according to Liu et al. (2017), have been showing strong growth in current times. Wind energy is seen as an excellent alternative to reduce damage to the environment, in addition to the immense availability of this energy source, considered inexhaustible. In this context, non-destructive testing techniques have contributed decisively to the quality control of wind turbine blades (Wind Turbine Blades - WTB) manufactured with composite materials.

With the advent of Industry 4.0, process automation and the replacement of man by machine have become a strong trend, attributing greater production speed and high reliability, which provides maximum quality to the final products. The concept of total quality has been a fundamental issue since the 1990s. Defect-free manufacturing, superior marketing of totally reliable products, increased productivity, elimination of unnecessary costs and adaptation of rejected products in the field are increasingly common policies adopted in the large industry.

According to Maldague (2001), one of the great challenges to reach the concept of total quality in production lines is the use of non-destructive tests with the implementation of computer vision. The automatic inspection eliminates the operator's fatigue and lack of motivation, frequent in manual inspections, avoiding the exhausting work of human beings.

Computer vision can be implemented in hostile environments, allowing for greater reliability, faster processes and reduced rework losses. Increasing quality reduces the number of defective parts, reducing manufacturing time.

Khodayar et al. (2017), Vavilov (2017) and Deane et al. (2019), report that infrared thermography has gained important prominence among non-destructive tests used in the quality control of composite materials in the civil, nuclear, aerospace, renewable energy, automotive, archeological, medical, and wind energy industries. Materials such as glass fiber reinforced polymer (GFRP) and carbon fiber reinforced polymer (CFRP) have excellent mechanical properties such as low density, light weight, high rigidity, tensile and compression strength, and also have good fatigue strength. These characteristics provide a good performance in wind turbine blades, as pointed out in several scientific articles.

During manufacturing, repair and operating processes, various types of failures can occur in composite wind blades, such as delamination, diffuse porosity or fiber matrix cracking. Applications of active thermography techniques are interesting on large and complex composite material surfaces because they are practical and easy to inspect. Thermographic methods are easy to detect failures using temperature response under thermal pulses, where results of excellent reliability are obtained. The induction of an external pulsed heat source followed by the capture of a sequence of thermograms allows detection of surface damage to the inspected sample. Digital thermographic image processing approaches and computer vision systems are widely discussed in terms of non-destructive testing. Li et al. (2018) and Avdelidis, Ibarra-Castanedo, Maldague (2013), note that infrared thermography (IRT) becomes one of the most promising technologies for presenting advantages such as no need for contact, fast inspection, excellent tolerance to curvature, quantitatively determines the extent and damage rate, provides real-time information, provides fast, cost-effective and reliable inspection for wind blade evaluation. Panella et al. (2020) state that active infrared thermography essentially involves the verification of mechanical properties and the detection of internal discontinuities and defects to investigate the integrity of the analyzed material.

Some typical damage to a WTB is during wind turbine operation due to wind, lightning, heavy rain, ice build-up, fatigue loads, insufficient mechanical strength of the blade material. Other failures occur due to human errors during the manufacturing processes and during the assembly of the wind turbine. The earlier it is detected, the lower the maintenance costs. Du et al. (2019) classifies WTB damage into four types: downwind skin damage, main spar outer surface damage, non-visible damage, main spar inner surface damage, trailing edge, leading edge, adhesive gasket on main stringer, main stringer. Li et al. (2018) highlights that damage to the blades is one of the most common in a wind generator, in addition, repairs to damage to the blades are more expensive and require a relatively longer time. The most common types of defects found in these regions are: adhesive joint failure, adhesive detachment, delamination, cracks, compression failure, among others.

Hidalgo-Gato et al. (2013) state that in the literature, several digital image processing techniques have been developed for active infrared thermography, integrated with other existing techniques, in order to successfully improve the detection of defects. Its application depends on the characteristics and objectives of the study, where the techniques can be simply classified into three groups: techniques that use thermal contrast, techniques based on transforms and techniques that use statistical methods.

Panella et al. (2020) emphasize that currently innovative thermal contrast processing methods are able to identify the limits of defects, by which they are automatically visualized in modified thermal contrast maps. These are optimized for better reconstruction of the defect shape to facilitate inspections over large areas even for small defects, similar to ultrasonic c-scans.

Lopez et al. (2013) explain that despite the advantages of Pulsed Thermography (PT), one of the difficulties concerns non-uniform heating due to the application of thermal/optical excitation, which is an intrinsic problem in the configuration of heat sources. Negative effects such as non-uniform heating lead to considerable limitations in inspection results due to the reduction in spatial resolution, which makes it difficult to detect smaller defects, as well as limiting the detection of deeper defects. Most of the problems arising from non-uniform heating can be considerably reduced by implementing signal processing techniques for the raw data obtained from a PT inspection. In Lopez et al. (2013) the implementation of thermographic signals reconstruction techniques.

A method called Pulsed Phase Thermography - PPT, developed for non-destructive testing in applications from just before the 21st century, is a starting point for promising alternatives for signal processing in infrared thermography, introduced in Madalgue and Marinetti (1996), as indicated in Madalgue et al. (2002).

In Lopez et al. (2013) the implementation of thermographic signal reconstruction techniques ou Thermal Signal Reconstruction - TSR, associated with Differential Absolute Contrast - DAC and Pulsed Phase Thermography - PPT aim to improve the reduction of the noise content in raw data, and their performances are compared, with respect to the effectiveness in quantifying the signal-to-noise ratio.

This work essentially proposes the implementation of a pulsed active thermography technique, based on concepts of the absolute thermal contrast method for the identification of artificial defects after the fabrication of a composite material of Fiberglass Reinforced Polymer (GFRP) used in the fabrication of wind turbine blades. For this, a computer vision system is implemented through OpenCV routines with the objective of detecting internal defects in the GFRP samples. This process basically consists of the implementation of pre-processing, segmentation and application of post-processing in thermograms with higher thermal contrasts, captured using an infrared camera. The following steps are performed in this process:

1) Fabricate Fiberglass Reinforced Polymer (GFRP) samples with artificial internal defects to analyze detectability by varying equivalent diameter and depth between composite layers.
2) Plan the experimental test in accordance with the norms and articles relating to infrared thermography tests on samples of the GFRP composite, applied with the aid of an infrared thermographic camera.
3) Adopt the pulsed thermography technique and absolute thermal contrast based on the thermograms obtained in the experimental test with the infrared camera.
4) Implement and test computer vision system algorithms from OpenCV library routines using Python programming language.
5) Apply the computer vision system to the sequence of thermograms of the experimental test, and analyze the detectability of internal defects in the samples according to the diameter "*D*" and depth "*z*" of the artificial defects and their respective "*D/z*" ratios.

2. GENERAL CONCEPTS OF THERMOGRAPHY TECHNIQUES

According to Maldague (2001), thermography is a type of non-destructive test that aims to analyze the temperature distribution on the surface of the body, and through this analysis the presence of surface defects and internal surface defects is observed. The detection is possible due to the change in the heat flux when there is a discontinuity in the material, resulting in surface temperature differences detectable by the infrared camera, which is considered the main defect detection mechanism by the thermography technique.

There are basically two ways in which thermography is classified: Passive (Conventional) Thermography or Active Thermography.

2.1 Passive Thermography

According to Maldague (2001), in passive or conventional thermography, the thermographic test is performed so that the inspected object emits the heat by which a thermographic camera detects the intensity of infrared radiation, enabling the observation of thermal contrast through the temperature gradient emitted spontaneously on the surface of the analyzed body, allowing the detection of excessive heat intensities in equipment with abnormal overheating in certain components.

Grinzato (2012) state that in this modality, the temperature measurement is carried out in the steady state, in which an external heat source is not applied to the inspected material to cause temperature variation. The defects themselves naturally emit a disproportionate amount of heat during the operation of the inspected object, with no need for external excitation to be detected.

Only one thermogram is needed in this modality, as there are no considerable changes in the temperature distribution of the inspected object during the acquisition time of the thermograms, as indicated by Grosso (2016). As examples of passive thermography, we consider the analysis of bearings, reducers, bearings of a shaft rotating at considerable speeds, a coupling between an electric motor and a pump in operation, electrical resistances or capacitors in an electronic circuit in operation. It is often possible to assess in passive thermography whether the inspected object is in operating condition or not.

In a thermographic image, a widely discussed concept is the thermal contrast, which is the temperature difference between a region without defects and another region with defects shown in thermograms captured by the infrared camera.

2.2 Active Thermography

Maldague (2001) explains that in active thermography the source of thermal excitation is external to the inspected body to induce a temperature difference (thermal contrast) between the defective region and the region without defects on its surface, that is, it causes, in this way, a variation in temperature over the observation time. The temperature measurement, in this case, is performed in the transient state in which the inspected object is subjected to a heating flow in a short period of time and cooling verification, which generates a temperature variation on the surface of the material along the cooling time. Thermograms are captured in which the temperature matrix represented by the pixels of the thermal image for each cooling moment is observed. Infrared sensors, when heated by infrared radiation, convert them according to radiant intensity, into current or voltage values, and the color of each pixel will be associated with a certain temperature of the radiation emitted by the body. Thus, the infrared camera captures infrared (non-visible) radiation and converts it into images visible to the human eye.

In active thermography, two ways to position the thermal source are commonly used: the reflection mode and the transmission mode. The reflection mode - exemplified in figure 1 - is more recommended to detect discontinuities close to the surface to be thermally excited, while the transmission mode is used to detect discontinuities that are located close to the surface opposite to the thermal excitation. When the opposite surface is not accessible, it is recommended to use reflection mode.

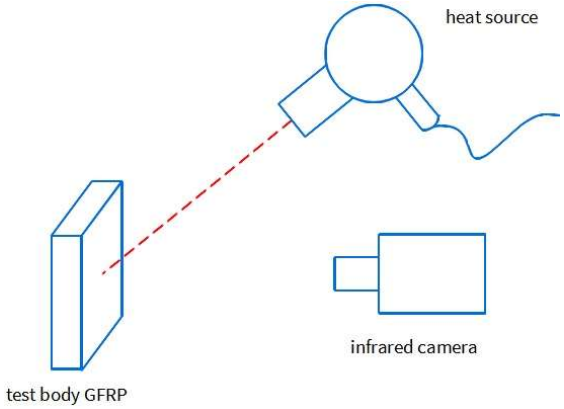

Figure 1. Example of a basic scheme active thermographic test in reflection mode.

The main thermal exciters in active thermography are: high power lamps, photographic flashes, hot air blowers, electrical resistors, lasers, ultrasonic beams, eddy currents, among others.

2.3 Pulsed Thermography and Absolute Thermal Contrast

In this pulsed active thermography technique, the excitation source consists of a short duration thermal pulse in which high conductivity materials (metals) receive a pulse of milliseconds, while low conductivity materials (polymers and composites) receive a pulse of a few seconds. Low conductivity materials do not allow sufficient penetration of heat into the body, thus limiting the detectable depth of the defect, according to Grosso (2016). This pulse generated by an external thermal excitation source causes a rapid increase in surface temperature due to the propagation of a thermal wave, which through diffusion penetrates into the inner layers of the material.

Maldague (2001) observes that when analyzing the sequence of thermograms generated by the infrared camera, it is possible to notice the change in the heat diffusion rate between a region where there are internal defects, and another region without internal discontinuities. Therefore, the region containing the discontinuity will appear as an area of different temperatures in relation to the rest of the material.

According to Khodayar et al. (2017), the absolute thermal contrast is defined as the temperature difference between a defect-free area and a defect area in the inspected object. In this technique, subsurface defects are detected by observing non-uniform changes in the heat diffusion rate shown in the thermogram sequence, where the temperature of a pixel or the average value of a group of pixels in a defective area is given by $Td_{[x,y]}(t)$ and the temperature in a defect-free area $Tref_{[x,y]}(t)$ is the temperature at time t for the non-defective area. An absolute thermal contrast history of these two pixels is the variable adopted to analyze the temperature distortion in a sequence of thermograms captured by the infrared camera.

A monitoring of the evolution of the thermal contrast in the pixels of the image temperature matrix versus the pulse propagation time during the warm-up to the cool-down of the test allows us to observe which is the defect where the absolute thermal contrast is maximum, which may be related to the influence of the relationship between the mean diameter and the depth of the defect in the detectability of the defect. Knowing that x and y are the pixel position coordinates, the equation that defines the absolute thermal contrast is given by:

$$C_{[x,y]}(t) = Td_{[x,y]}(t) - Tref_{[x,y]}(t) \quad (1)$$

Where $C_{[x,y]}(t)$, $Td_{[x,y]}(t)$, e $Tref_{[x,y]}(t)$ are absolute thermal contrast, temperature the pixel in the region of the defect, and the temperature in the reference pixel, respectively. The coordinates of pixel position and thermal pulse time are given by x, y, t, respectively.

The external heat source heats the surface of the object for a brief period of time by interrupting the heat flow. After interruption of the excitation source, the material cools, reaching a maximum difference between the temperatures $Td_{[x,y]}(t)$, and $Tref_{[x,y]}(t)$ in an instant of time called t_{pico}. This is the instant at which the absolute thermal contrast reaches a maximum value, as shown in Figure 2.

Grosso (2016) states that the temperature curves and absolute thermal contrast over time, obtained for each specimen during heating and cooling, are an important tool to estimate the influence of the size and depth of defects in the analysis of the level of detectability of the thermographic test.

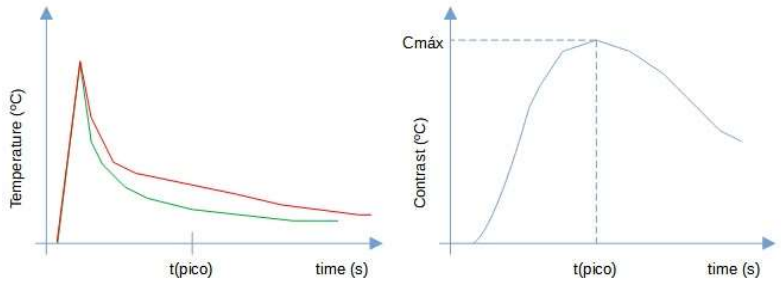

(a) (b)

Figure 2. Examples of graphs (a) of temperature vs time for a pixel in the defect region – red, and another pixel in the defect region – green; (b) the evolution of absolute thermal contrast vs time for the analyzed defect (Maldague, 2001).

The influence of the defect depth on the thermal contrast level is related by the peak time equation for the maximum thermal contrast reached, as indicated in Maldague (2001).

$$t_{pico} \approx {z^2}/{\alpha} \quad ; \quad C \approx {1}/{z^2} \ , \tag{2}$$

where, t_{pico} , and C are the peak time of thermal contrast (s) and thermal contrast, respectively, and z, α, are depth of discontinuity (m), and thermal diffusivity of the material (m²/s), respectively.

Madruga et al. (2010) state that a wide variety of techniques are applied to pulsed thermographic data for analysis of raw data captured by thermographic cameras. Fourier, Hough, Radon transforms can be used with the purpose of using alternative domains in data analysis. Moradi and Safizadeh (2019) observe that the thermal signal reconstruction (TSR) technique was developed for pulsed thermography in order to process the temperature history of each pixel from the sequence of thermographic images. TSR is based on the assumption that temperature profiles for non-defective pixels must follow the approximate one-dimensional (1D) solution of a logarithmic Fourier equation, where the thermal signal reconstruction (TSR) stores the $n + 1$ coefficients of a polynomial of n degrees, which fits the decay curve of each pixel into a double logarithmic space. However, to adjust the approximate solution, the logarithmic time response is linearized with the polynomial function of degree n in equation 3:

$$ln\left(T(t)_{[i,j]}\right) = a_0 + a_1 ln\,(t) + a_2[ln(t)]^2 + \ldots + a_n[ln\,(t)]^n \tag{3}$$

Where, $T(t)_{[i,j]}$ is the temperature increase as a function of time for each pixel of position *[i, j]*, and a_0 *[i, j]*, a_1*[i,j]*,…, a_n *[i, j]* are the polynomial coefficients, also in position *[i, j]*. The TSR approach detects smaller, deeper defects because this method provides significant improvements in noise reduction.

Statistical parameters such as principal component thermography (PCT), performance of higher-order statistic (HOS) parameters are also techniques employed in pulsed thermography showing high levels of defect contrast in relation to raw data, as indicated by Madruga et al. (2010).

3. MATERIAL AND METHODS

3.1 Preparation of GFRP samples and apparatus for experimental testing

To carry out the experimental test, it is necessary to manufacture three samples of GFRP. First, the molds are dimensioned in AutoCAD, and they are 3D printed. The basic dimension of the specimen to reference the molds is a length and width of 120 x 120 mm and a z-thickness of 10 mm. For a better visualization of the processes for making the GFRP samples, follow the steps indicated in the figure 3.

The specimens are composed of layers of chopped fiberglass yarn mat and Fortcom 3100 polyester resin with 2% tecnox super catalyst. The defects included in the three samples are small squares of cardboard covered with adhesive tape that vary in their equivalent diameters. Considering an equivalent diameter "*D*" equal to the side of a perfect square "*l*", such that "*D = l*", three types of equivalent diameters are determined, 6 mm, 8 mm and 10 mm, in which it varies the different depths between the layers of composite material samples. The "*z*" depths are estimated with the number of layers of composite (fiberglass and resin), each layer of mat plus resin being approximately 1.5 mm.

The external heat source is a hot air blower that can reach a maximum power of 2000 W, in which the air temperature is measured in the settings of the experimental test with thermocouples. Blower air flow velocities are measured with an

anemometer and offer two air flow possibilities. The apparatus for the thermographic test will be configured in transmission mode, as indicated in figure 1 of sub item 2.2.

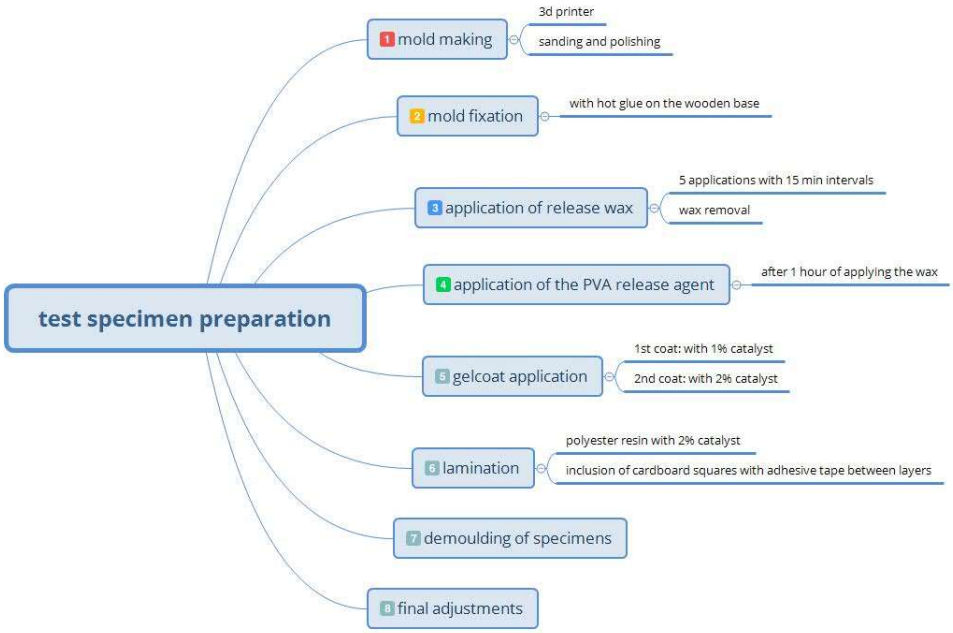

Figure 3. Sequence of steps for making GFRP samples.

The non-destructive testing standard ABNT NBR 15572:2013 presents a Guide for the inspection of electrical and mechanical equipment, for thermographic testing. This standard is useful for the preliminary parameter settings of the infrared camera when carrying out the experimental test. According to the aforementioned standard, for the specification of the appropriate instrument, it is recommended that, according to the application, the user observes the following items:

a) measuring temperature range;
b) spectral range;
c) spatial and measurement resolution;
d) type of detector;
e) thermal sensitivity;
f) field of view (FOV);
g) frame rate;
h) operating temperature;
i) degree of protection of the instrument: electromagnetic interference, resistance to vibrations and shocks, encapsulation;
j) physical characteristics: ergonomics, weight, dimension;
k) possibility of adjusting parameters: distance, temperature and humidity, emissivity;
l) post-processing that allows a qualitative and quantitative assessment based on the change in measurement parameters;
m) calibration certificate with recognized traceability.

The infrared camera used in the thermographic test of model FLIR E4 1.0 was configured for an emissivity value of 0.8, as it is the closest value allowed by the camera, for GFRP polyester resin specimens with an emissivity of approximately 0.9. Focusing distance used was 0.3 m.

3.2 Methodology flowchart

In planning the experimental test, the following steps are carried out:

I) literature review involving articles about pulsed thermography, absolute thermal contrast, computer vision systems and thermographic image processing.

In the thermographic experimental test, the following is carried out:

I) sample preparation;
II) configuration of the experimental apparatus in transmission mode;

III) determination of thermal pulse times from infrared camera parameters, observation and necessary adjustments until finding the appropriate conditions for the test;
IV) execution of the experimental test.

In the computer vision system and digital thermographic image processing, the following steps are performed:

I) Identification of the position of pixels in the thermogram temperature matrix in areas with and without defects;
II) Identification of the maximum thermal contrast thermograms for the three samples;
III) Implementation of digital image processing and computer vision algorithms to automate the process of detecting and quantifying artificial internal defects in GFRP samples.

The flowchart chart of the work methodology can be seen in Figure 4:

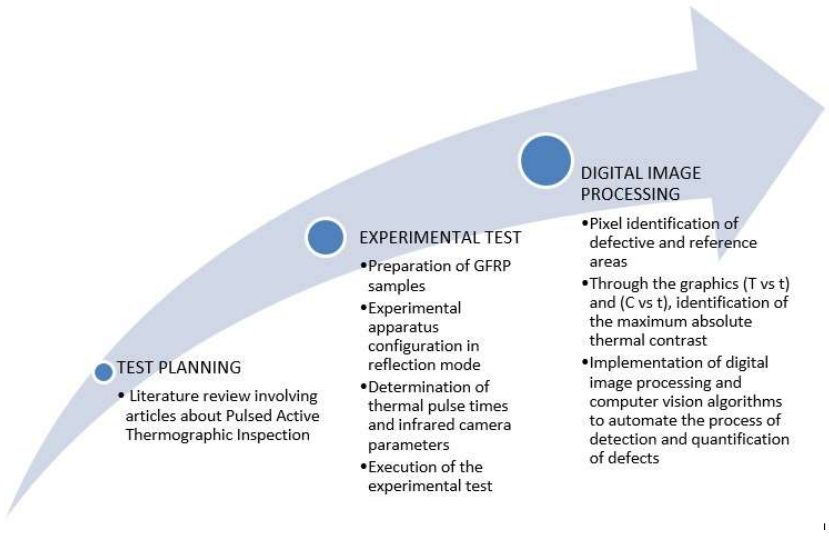

Figure 4. Work methodology flowchart.

The methodology for implementing the digital thermographic image processing is more clearly detailed in the flowchart in Figure 5 and is explained in greater detail in the item of expected results and discussion.

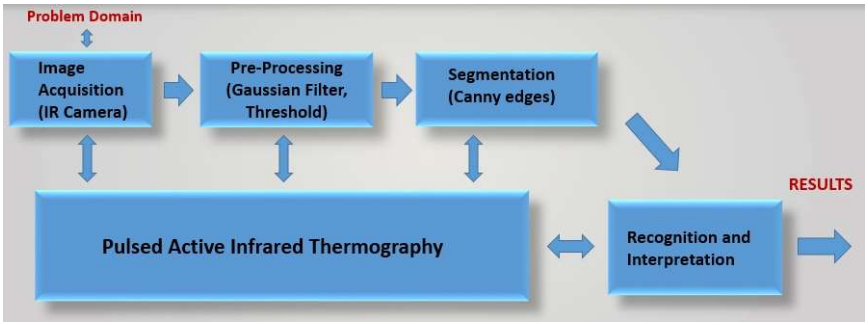

Figure 5. Implemented digital image processing methodology, adapted from Digital Image Processing, Gonzalez, Woods (2019).

4. RESULTS AND DISCUSSION

The GFRP samples are shown in Figure 6. The artificial defects included between the layers of the GFRP composites are located between the first and tenth layers, considering the first layer as the upper surface, and the last layer as the lower surface. Each composite layer had a thickness or depth of approximately 0.8 mm. In sample 1, defects are in the first, second and third layers. In sample 2, the defects are in the fourth, fifth and sixth layers and in sample 3, the defects are in the seventh, eighth and ninth layers.

It is noteworthy that the three samples numbered 1, 2 and 3 must present, as already mentioned, internal defects of square shape presenting three different equivalent "D" diameters of 6, 8 and 10 mm for each layer of the compound, and depths "z" estimated according to the number of layers, as shown in Table 1. Thus, a relationship "D / z" is presented for each defect, as can also be seen in Table 1. From this method, it is possible to establish a relationship for the detectability efficiency in the processing of the thermogram images implemented in this work.

Figure 6. GFRP composite samples 1, 2 and 3 from left to right, respectively.

Table 1. Values related to the composite layers of the GFRP samples and the *D* diameters, *z* depths of the artificial defects, in addition to their respective *D/z* ratios.

Layers	**1st**	**2nd**	**3th**	**4th**	**5th**	**6th**	**7th**	**8th**	**9th**	**10th**
z (mm)	0.8	1.6	2.4	3.2	4	4.8	5.6	6.4	7.2	8
D (mm)	**Diameter to Depth Ratio (D/z)**									
6	7.50	3.75	2.50	1.87	1.50	1.25	1.07	0.94	0.83	-
8	10	5	3.33	2.50	2	1.67	1.43	1.25	1.11	-
10	12.5	6.25	4.17	3.12	2.50	2.08	1.78	1.56	1.39	-

The experimental test was carried out in order to present the thermographic images where the highest thermal contrasts observed between several images captured during the cooling of the samples were presented. A hot air blower was activated for 20 seconds, generating a flow of heat over the surface of the samples to capture images with the infrared camera right after the heat was supplied. Images were captured at approximately two-second intervals. The digital processing of thermogram images was implemented with the help of routines from the OpenCV library of the Python programming language, in order to detect regions where there is discontinuity in the heat flow observed on the surface of the inspected specimen. In the first preprocessing, a pixel positioning matrix and preprocessing with a Gaussian filter are implemented to remove image noise from the thermograms shown in Figure 7. A Gaussian filter is used to blur or blur the image that is applied in order to reduce the noise present in the image.

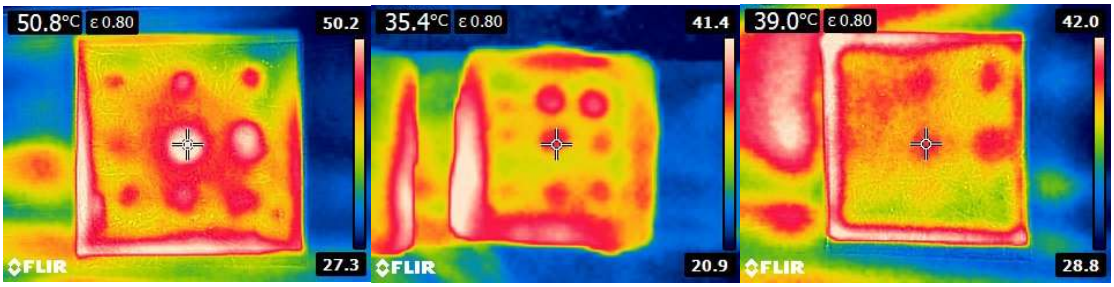

Figura 7. Higher absolute thermal contrast thermograms of samples 1, 2 and 3, from left to right, respectively.

The second pre-processing consists of transforming the image from RGB to grayscale to implement an image binarization in order to separate regions with the greatest discontinuities in the heat flow in the thermographic image.

A segmentation with a Canny edge detector is applied in which regions of high energy are highlighted by contours for a better visualization and quantification of the regions where there is greater discontinuity in the observed heat flux. Thus, it is possible to detect internal defects where the greatest variations in the heat flux occur, indicating the presence of internal discontinuities on the sample surface.

A better detection will be possible after the final finishes of the specimens. The unevenness of the external surface, that is, the lack of flatness and the lack of a better surface finish of the samples resulted in an excessive concentration of heat at the edges and in other regions around the artificial defects, making their identification difficult. Vacuum infusion is the recommended manufacturing process for better surface finish of samples. Another important factor is the application of the heat flow in a well-distributed way in the sample, as a duct is needed to better distribute the hot air flow on its surfaces.

The values of the *D/z* ratio shown in green in Table 1 are of good detectability by the implemented digital image processing, as seen in Figure 8. The values in red, on the other hand, did not show good detectability. It appears that the greatest difficulties in detecting artificial defects occur at *z* depth values of 4.8 mm for an apparent diameter *D* of 6 mm. For diameters of 8 and 10 mm, detection difficulties only from 7.2 mm in depth. It is observed that defects with a lower

"*D / z*" ratio presented greater difficulties in detection. For values below 1.39, greater difficulties were observed, and values above 1.39 are possible detection by the digital image processing presented.

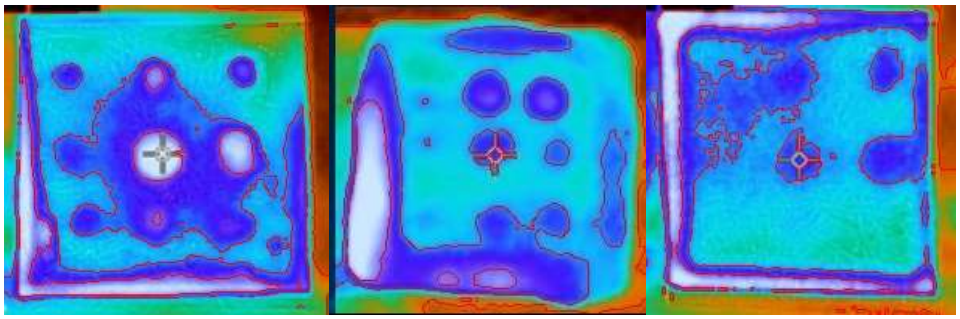

(a) (b) (c)

Figure 8. Segmentation and recognition of samples 1, 2 and 3, in a, b and c respectively.

Thus, the first results are presented from the implementation of algorithms for digital processing of the thermographic image of the three GFRP samples of the experimental test carried out.

5. CONCLUSION

In this study, the possibility of applying the pulsed active thermography technique through non-destructive tests for considerable thicknesses of GFRP is verified, in order to contribute immensely in the quality inspection processes used in the manufacture of wind blades, being able to attribute greater speed and reliability in thermographic inspection processes.

In this work, it was found that it is possible to apply digital image processing together with pulsed thermography and absolute thermal contrast techniques for composite materials, although improvements are needed with other techniques such as TSR, PCT or HOS to automate this process and obtaining improvements in the detection of internal defects of the GFRP material.

The results presented indicate that a final finish on the specimens is necessary to provide greater uniformity of heat rates in regions without defects, as the unevenness of the surface of the sample caused overheating at the ends, making the implemented evaluation of artificial defects difficult. Non-uniformity of heat flow can also result in difficulties in detecting defects.

The experiments with samples of this GFRP compound have the function of analyzing and evaluating artificial internal defects of the inspected material, in which, after carrying out the experimental test, it was possible to prove the possible effectiveness of the techniques presented, with some small adjustments in the test. In addition, an evaluation of the effect of the relationship between diameters and depths was carried out, showing the good detection potential of thermography for thicknesses of 10 mm of the GFRP composite material.

6. REFERENCES

Maldague, X., Galmiche, F., Ziadi, A., 2002. “Advances in pulsed phase thermography”. *Infrared physics & technology*, Vol. 43, n. 3-5, p. 175-181.

Maldague, X., Marinetti, S., 1996. “Pulse phase infrared thermography”. *Journal of applied physics*, Vol. 79, n. 5, p. 2694-2698.

Maldague, X., 2001. “Theory and practice of infrared technology for nondestructive testing”. *John Wiley & Sons*, New York.

Liu, Q. X., Wang, Z. H., Long, S. G., Cai, M., Wang, X., Chen, X. Y., & Bu, J. L., 2017. “Research on Automatic Positioning System of Ultrasonic Testing of Wind Turbine Blade Flaws”. In *IOP Conference Series: Earth and Environmental Science*, Vol. 93, No. 1, p. 012074. IOP Publishing.

Wei, Y., Zou, Q. P., & Lin, X., 2021. “Evolution of price policy for offshore wind energy in China: Trilemma of capacity, price and subsidy”. *Renewable and Sustainable Energy Reviews*, Vol. 136, p. 110366.

Khodayar, F., Lopez, F., Ibarra-Castanedo, C., & Maldague, X., 2017. “Optimization of the inspection of large composite materials using robotized line scan thermography”. *Journal of Nondestructive Evaluation*, Vol. 36, n. 2, p. 32.

Li, Xiao-li et al., 2018. “An Effective Method to Inspect Adhesive Quality of Wind Turbine Blades Using Transmission Thermography”. *Journal of Nondestructive Evaluation*, Beijing.

Avdelidis, N. P.; IBARRA-CASTANEDO, C.; MALDAGUE, X. P. Vol., 2013. “Infrared thermography inspection of glass reinforced plastic (GRP) wind turbine blades and the concept of an automated scanning device”. In *Thermosense: Thermal Infrared Applications XXXV*, *International Society for Optics and Photonics*. p. 87050G.

Panella, F. W., Pirinu, A., & Dattoma, V., 2020. "A Brief Review and Advances of Thermographic Image-Processing Methods for IRT Inspection: A Case of Study on GFRP Plate". *Experimental Techniques*. p. 1-15.

Du, Y., Zhou, S., Jing, X., Peng, Y., Wu, H., & Kwok, N., 2020. "Damage detection techniques for wind turbine blades: A review". *Mechanical Systems and Signal Processing*, Vol. 141, p. 106445.

Grinzato, E., 2012. "Thermal Non-Destructive Testing and Evaluation". In 18th World Conference on Non Destructive Testing, Durban, South Africa.

Vavilov, V. P., 2017. "Thermal nondestructive testing of materials and products: a review". *Russian Journal of Nondestructive Testing*, Vol. 53, n. 10, p. 707-730.

Deane, S. et al., 2019. "Application of NDT thermographic imaging of aerospace structures. Infrared Physics & Technology". Vol. 97, p. 456-466.

Hidalgo-gato G. R. et al., 2013 "Quantification by signal to noise ratio of active infrared thermography data processing techniques". *Optics and Photonics Journal*. 03(04), p. 20-26. Cantabria, Spain.

Lopez, F., Ibarra-Castanedo, C., Maldague, X., & de Paulo Nicolau, 2013. "Analysis of signal processing techniques in pulsed thermography". In *Thermosense: Thermal Infrared Applications XXXV*, International Society for Optics and Photonics. Vol. 8705, p. 87050W.

Grosso, M. *Detecção de defeitos em aços com revestimentos anticorrosivos através da técnica de termografia aliada ao emprego de simulaçao computacional*. 2016. Doctoral Dissertation. Program of M. Sc. in Metallurgical and Materials Engineering, Federal University of Rio de Janeiro, Rio de Janeiro, Brazil.

Madruga, F. J. et al., 2010. "Infrared thermography processing based on higher-order statistics". *NDT & E International*, Vol. 43, n. 8, p. 661-666.

Moradi, M., Safizadeh, M. S., 2019. "Detection of edge debonding in composite patch using novel post processing method of thermography". *NDT & E International*, Vol. 107, p. 102153.

Gonzalez, R. C., Woods, R. E., 2000 "Processamento de imagens digitais". Editora Blucher.

7. RESPONSIBILITY NOTICE

The authors Júlio César Capistrano Estácio, Darlan Almeida Barroso, Marcello Carvalho dos Reis, Jessyca Almeida Bessa and Auzuir Ripardo de Alexandria are the only responsible for the printed material included in this paper.